JOURNAL OF AGRICULTURAL AND FOOD CHEMISTRY

Article

Carotene reactivity in pink grapefruit juice elucidated from model systems and multi-response modelling

Nawel Achir, Thiziri Hadjal, Khodir Madani, Manuel Dornier, and Claudie Dhuique-Mayer

J. Agric. Food Chem., **Just Accepted Manuscript** • DOI: 10.1021/acs.jafc.5b00509 • Publication Date (Web): 30 Mar 2015

Journal of Agricultural and Food Chemistry is published by the American Chemical Society. 1155 Sixteenth Street N.W., Washington, DC 20036

Carotene reactivity in pink grapefruit juice elucidated from model systems and multi-response modelling

Nawel Achir[1*], Thiziri Hadjal[2,3], Khodir Madani[3], Manuel Dornier[1], Claudie Dhuique-Mayer[2]

[1]Montpellier SupAgro, UMR95 QualiSud, 1101 av. Agropolis, B.P. 5098, F-34093 Montpellier cedex 5, France

[2]CIRAD, UMR95 QualiSud, 73 av. J.F Breton, TA B-95/16, F-34398 Montpellier cedex 5, France

[3]Laboratoire de Biomathématique, Biophysique, Biochimie, et Scientométrie, Faculté des Sciences de la Nature et de la Vie, Université de Bejaia, 06000 Bejaia, Algeria

***Corresponding author:**

nawel.achir@cirad.fr

Tel. +33 (0) 4 67 87 40 89 or +33 (0) 4 67 61 55 47

Fax. +33 (0) 4 67 61 70 55

Abstract: This study was carried out to assess the impact of the pink grapefruit juice composition and structure on the degradation kinetics of lycopene and β-carotene using model systems and multi-response modelling. Carotenes were heated at four temperatures in their native matrix (juice) or extracted and incorporated in water/ethanol emulsion systems formulated with or without ascorbic acid or naringin. Kinetic analysis showed that the rate constants and activation energy were lower for lycopene than for β-carotene in the juice, while this trend was inversed in the model system. Multi-response modelling was used to analyze the role of ascorbic acid and naringin in carotene degradation. Ascorbic acid had a very low impact while naringin significantly increased the carotene degradation and isomerization rates. We concluded that lycopene was more sensitive to thermal degradation and phytochemical interactions than β-carotene, but this behaviour was masked in the fruit juice matrix by better structural protection.

keywords: β-carotene; lycopene; *citrus* fruit; kinetic; naringin; ascorbic acid.

Introduction

Pink grapefruit (*Citrus paradisi* Macf.) with its red flesh color is a lycopene pigmented citrus. This fruit is consumed worldwide and is a rich source of micronutrients (minerals, vitamin C, folic acid) and phytochemicals such as flavonoids and carotenoids [1]. The nutritional value of citrus fruits is now well established in the prevention of and/or protection against several human diseases [2]. Due to its flavonoid content, pink grapefruit is particularly involved in the hypocholesterolemic effect on laboratory animals and in hypocholesterolemic patients [3, 4].

The carotenoid profile of grapefruit juice is simple, with two major carotenoids which are nonpolar hydrocarbons: β-carotene and especially lycopene [5]. Xu *et al.* (2006) report a ratio of 3 between lycopene and β-carotene in red fleshed grapefruit, with contents of 283 and 93 µg/g dry basis, respectively [6]. These carotenoids are important from a nutritional standpoint. β-carotene is a provitaminic A carotenoid and there are literature reports that lycopene is a bioactive compound of dietary importance which is also detectable in human plasma. Both *in vitro* and *in vivo* studies on animals and cell cultures have suggested that lycopene has anticarcinigenic and anti-atherogenic effects [7]. Since β-carotene has the highest vitamin activity among carotenoids, its degradation has been widely studied at the mechanistic and kinetic level. This molecule is subjected to isomerization and oxidation, followed by cleavage because of its unsaturated structure, particularly under the influence of heat and light during processing or storage. The main degradation products identified are *cis*-isomers, mainly 13-cis- and 9-cis-β-carotene [8, 9], epoxy carotenoids, apocarotenals [10] and aroma compounds [11]. Degradation of this molecule is mainly described by one-order kinetics and degradation rate constants are available for a large number of matrixes [12]. The rate constants and activation energies identified were found to be very dependent on the matrix. For instance, the degradation rate constant was 0.6 min^{-1} for orange juice at 90°C, 0.01 min^{-1} for citrus juice at

100°C and 0.006 min^{-1} in papaya puree at 105°C. There was also a marked discrepancy between the activation energy values, with 53 $kJ.mol^{-1}$ found in orange juice, 110 $kJ.mol^{-1}$ in citrus juice and 21 $kJ.mol^{-1}$ in papaya puree [13-15].

Lycopene has been less studied. It also has 11 conjugated double bonds but, contrary to β-carotene, it is an acyclic carotenoid. It is more susceptible to degradation via isomerization because of this less steric hindrance. Consequently, in comparison to β-carotene, a higher number of *cis* geometrical isomers were formed under processing or storage conditions [16]. By the use of quantum chemistry computations, Guo *et al.* (2008) suggested that the following isomers were thermodynamically favored at room temperature, in the following order: all-*trans* > 9-*cis* > 13-*cis* > 15-*cis*. In tomato matrices, the main *cis* isomers found were 5-*cis*, 9-*cis*, 13-*cis* and 15-*cis* lycopene and they were also found in human serum [17]. Moreover, several di-*cis*-isomers were identified in processed tomato products [18]. Recently, Xu and Pan (2013) found that 9, 13'-di-*cis*, 9, 13-di-*cis*, 15-*cis*, 13-*cis*, and 9-*cis*-lycopene were formed during ultrasonic treatment extraction of all-*trans*-lycopenes from red grapefruit [19].

Kinetic parameters are less available for lycopene. Most studies also use a one order degradation model to identify kinetic data. In model systems, degradation rate constants at 100°C were 0.0124 min^{-1} for lycopene standard [20] and 0.0024 min^{-1} in octyl/decyl glycerate [21]. In real matrix, Goula *et al.* (2006) found 0.0012 min^{-1} in tomato pulp at 90°C [22] and Sharma *et al.* (2008) found 0.0048 min^{-1} in watermelon at the same temperature [23]. Colle *et al.* (2012) found a much higher degradation rate constant at 100°C (0.095 min^{-1}), but in a formulated tomato and oil emulsion [24]. Activation energies found in model systems were 61 $kJ\ mol^{-1}$ [20]and 77 $kJ\ mol^{-1}$ [21]. In real matrix, lycopene activation energies were 19.5 and 26.4 $kJ\ mol^{-1}$ in tomato and watermelon, respectively [22, 23]. Colle *et al.* (2013) found an activation energy of 28 $kJ\ mol^{-1}$ in tomato pulp/olive oil emulsion. These results show that the kinetic parameters of lycopene degradation are also significantly different as a function of the food

system, which could be due to the strong influence of the chemical environment and the inclusion of carotenes in complex structures. To overcome this matrix effect, some authors finally proposed to formulate juice-like system with controlled composition, but which could be complexified progressively to gain greater insight into the effect of the chemical and structural environment and obtain better accuracy on the kinetic parameters. Zepka *et al.* (2009) designed a cashew apple juice model based on a water and ethanol mixture [25]. A more recent study of Hadjal *et al.* (2013) [34] assessed the degradation kinetics of xanthophylls from blood orange in both real and model matrices. They showed that the degradation rates were the lowest in real juice compared to the juice-like model. These authors suggested that phytochemical compounds of juice were able to protect xanthophylls, especially at high temperatures.

Kinetic uni-response models mentioned above are commonly used because they are robust and useful to predict nutrient loss. Kinetic modelling studies of both carotenoid degradation (oxidation and cleavage) and production of neoformed compounds such as isomers are more limited. This approach implies the use of more a sophisticated kinetic model or mathematical tools such as multi-response modelling [26-28]. However, knowledge on degradation and production rates could be of great interest to predict nutrient loss as well as neoformed compound production. Indeed, products generated during carotenoid degradation may have positive or negative biological activity. In addition, the knowledge of the impact of temperature on kinetic constants may help technologists improve thermal processes such as pasteurization. Besides the prediction advantages, this approach could provide insight into the degradation reaction scheme. Particularly, the use of multi-response modelling was used to enhance the comprehension of β-carotene degradation in oils [27] or in orange-fleshed sweet potato [28]. The principle of such an approach is to enable simultaneous study of analytical and literature results so as to be able to draw up possible observable degradation schemes that

could be expressed mathematically. The most probable hypothesis can be chosen by discrimination of the best kinetic model, i.e. the model which presents the closest fit to the experimental data.

Consequently, the objectives of this study were to assess the degradation and isomerization kinetics of lycopene and β-carotene from pink grapefruit during heating, both in their natural matrix (juice) and in three different model systems (buffered water/ethanol basis) without or with the addition of ascorbic acid or naringin to simulate major antioxidant phytochemical compounds of pink grapefruit juice [1]. Moreover, multi-response modelling is applied to model simultaneous lycopene/β-carotene loss and isomerisation during thermal treatment.

Material and methods

Grapefruit juice

South American pink grapefruits (*Citrus paradisi* Macf) purchased in a market were cut in half and squeezed using a domestic juicer (Moulinex Masterchef 470, France). The juice was then filtered through a stainless steel sieve (1 mm). The freshly pressed juice was placed in amber glass bottles under nitrogen and stored at -20°C until analysis or heat treatment.

Preparation of juice-like model systems

Juice-like model systems were formulated with grapefruit juice carotenoid extract to carry out a degradation test in controlled medium. This extract was formulated with three media: acidified aqueous medium (AM), acidified aqueous medium supplemented with ascorbic acid (AM+AA) or naringin (AM+NAR)), which are major citrus juice phytochemicals that could have a protective effect.

Preparation of carotenoid extract: The first carotenoid extraction step was performed according to Dhuique-Mayer *et al.* (2005) by blending 80 g of grapefruit juice with an ethanol/hexane mixture (4/3, v/v, 0.1% BHT). The hexane fractions were collected, pooled and evaporated for 15 min at 20°C (GeneVac® EZ-2 compatible, UK). The carotenoid extracts obtained were used to formulate the three model systems [29].

Formulation of model systems: The model system was inspired from that of Zepka *et al.* (2009) [25]. It first involved solubilization of carotenoid extracts in ethanol. A pH 3 citrate buffer mixture was added at an ethanol/buffer ratio of 25/75 (v/v). This was called the acid medium (AM). The resulting model system was a very homogenous and stable cloudy liquid, even at high temperature. This mixture was assumed to be a spontaneous micro-emulsion, which is typically obtained when mixing hydrophobic molecules dissolved in ethanol with water. For AM+AA medium, the ethanolic carotenoid extract was mixed with citrate buffer supplemented with ascorbic acid in the same proportion (25/75, v/v). For AM+NAR medium, naringin was first dissolved in ethanol and mixed with 75% (v/v) citrate buffer. The amount of naringin and ascorbic acid added were calculated to obtain a content equivalent to that reported in the literature for pink grapefruit juice (300 mg L^{-1} for naringin and 400 mg L^{-1} for ascorbic acid) [1].

Heat treatment

The kinetics of carotene thermal degradation were assessed at four temperatures, i.e. 60, 75, 90 and 95°C. These temperatures cover the pasteurization treatment range involving low to high temperature (flash) treatments. For each temperature, 2 mL of grapefruit juice or model medium were heated in sealed 10 mL Pyrex tubes. The tubes were immersed in an oil bath with temperature control (Memmert, Legallais, France). A digital temperature probe (EKT 3001, Heidolph, Germany) fitted to a reference tube was used to measure the medium

159 temperature during the thermal experiments. Five sampling points were selected from 5 to
160 300 min according to the temperature. Three replicates were done for each temperature. The
161 time for juice to reach the set temperature was less than 4 min, and the cooling time was about
162 1 min in an ice water bath. The thermal transient could thus be neglected and the treatment
163 could be considered isothermal. Each tube was stored under nitrogen at -20°C until analysis.
164
165 **HPLC analysis of carotenoids**
166 **Sample preparation:** 2 mL of grapefruit juice were extracted with the ethanol/hexane
167 mixture (4/3; v/v). 20 µl of internal standard (apocarotenal) were added in order to estimate
168 carotene losses during the manipulations. The mixture was shaked for 30 s and centrifuged for
169 7 min at 2400 g. Four extractions were performed with 2 mL of hexane. The hexane fractions
170 were pooled and then evaporated for 15 min (GeneVac® EZ-2 compatible, UK). In the case
171 of model systems (AM+AA and AM+NAR), 2 ml were extracted three times with 1 mL of
172 hexane and the pooled hexane fraction was evaporated using the same procedure. All final
173 extracts were solubilized in 500 µL MTBE/methanol/dichloromethane (40/10/50, v/v/v)
174 before HPLC injection.
175 **HPLC analysis:** Carotenoids were analyzed by reverse-phase HPLC using an Agilent®1100
176 system (Massy, France) according to Dhuique-Mayer *et al.* (2007) [14]. The carotenoids were
177 separated using a C30 column (250 mm x 4.6 mm, 5 µm YMC) (Europ GmbH, Germany),
178 and the mobile phase was H_2O as eluent A, methanol as eluent B, methyl tert-butyl ether as
179 eluent C. The flow rate was set at 1 mL min^{-1}, the column was cooled to 15°C, and the
180 injection volume was 20 µL. A solvent gradient was programmed as follows: initial
181 conditions 40% A-60% B; 0-7 min, 20% A-80% B 7-10 min, 4% A-81% B-15% C 10-60
182 min, 4% A-11% B- 85% C 60-71 min, 100% B 71-72 min, with a return to the initial
183 conditions for rebalancing. β-carotene and lycopene and their isomers were detected at 450

and 470 nm, respectively, using an Agilent® photodiode array detector. Obvious carotenes were quantified on the basis of their calibration curve at the same wavelengths.

Determination of ascorbic acid in real juice and a model system

Ascorbic acid was determined by HPLC according to Dhuique-Mayer *et al*. (2005) [29]. Grapefruit juice or model juice (2 mL) were homogenized with 4 mL of a 4.5% metaphosphoric acid solution. Extractions were carried out in triplicate. After centrifugation, the supernatant was filtered through a 0.45 µm membrane and analyzed by HPLC using an Agilent model 1100 system equipped with an RP 18e Licrospher 100 (5 µm) column (250 mm x 4.6 mm id) (Merck KgaA, Darmstadt, Germany). The isocratic solvent system was a 0.01% solution of H_2SO_4, the flow rate was 1 mL min^{-1}, and detection was set at 245 nm. Ascorbic acid was quantified by the external standard method.

Determination of naringin in real juice and a model system

Naringin was determined by HPLC according to Dhuique-Mayer *et al.* (2005) [29]. Briefly, 5 mL of juice was homogenised with 10 mL of dymethylformamide and 10 mL of ammonium oxalate (0.05 M). Then the mixture was heated for 10 min at 90°C. After cooling, the volume was completed with distilled water to 50 mL, centrifuged (1000 g, 3 min) and the supernatant was filtered (0.45 µm). The HPLC analysis was carried out with an Agilent 1100 model system (Massy, France) using an RP 18e Licrospher® 100 (5µm) column (250 mm x 4.6 mm id) (Merck KgaA, Darmstadt, Germany). The isocratic solvent system was water/acetonitrile/THF/acetic acid (80:16:3:1, v/v/v/v). Quantification was carried out at 280 nm. The flow rate was set at 1 mL min^{-1}. Naringin concentrations were determined using an external calibration method.

209 **Numerical analysis of kinetic data**

210 **Carotene degradation in real juice and model media**

211 Carotene changes over time can be described by equation 1.

212 $$\frac{d[X]}{dt} = -k[X]^{\alpha} \qquad (1)$$

213 where [X] represents the carotene mass concentration (kg m^{-3}), t the time (s), k the reaction
214 rate constant ($kg^{(1-\alpha)}\, m^{3(\alpha-1)}\, s^{-1}$), and α the apparent reaction order.

215 The rate constants k were assumed to vary with the temperature according to the Arrhenius
216 equation:

217 $$k = k_{ref} \exp\left(\frac{-E_a}{R}\left(\frac{1}{T} - \frac{1}{T_{ref}}\right)\right) \qquad (2)$$

218 where k_{ref} is the rate constant at the reference temperature chosen in the middle of the studied
219 temperature range (80°C), with Ea, T and R respectively denoting the activation energy (J
220 mol^{-1}), medium temperature (K) and gas constant (8.314 J mol^{-1} K^{-1}).

221 The reaction order was determined by incrementing α in Eq. 1. Kinetic constants and
222 activation energies were identified by non-linear least square regression using the Levenberg-
223 Marquardt least square minimization procedure with Matlab® software (Mathworks Inc.,
224 Natick, Mass, USA).

225 **Multi-response modelling of the thermal degradation of carotenes in real juice and**
226 **model media**

227 Carotenes and their isomers were monitored during heat treatments. Carotenoids were
228 subjected to degradation, which could lead to other molecules that were not monitored by
229 HPLC and were therefore missing species. These missing products were evaluated by mass
230 balance.

231 Observable reaction schemes were proposed based on experimental observations and
232 literature data. When a reaction scheme was established, it was translated into a system of
233 differential equations and the kinetic parameters were optimized with the Levenberg-
234 Marquardt algorithm using Matlab® software (Mathworks Inc., Natick, Mass, USA).

235 **Model discrimination**

236 To discriminate the appropriate kinetic model under mono-response (reaction order) or multi-
237 response (most probable reaction scheme) conditions, the residual sum of squares (RSS) was
238 calculated according to equation 3. RSS measured the discrepancy between the experimental
239 and simulated data. A small RSS indicated a suitable goodness of fit of the model to the data.

240 $$RSS = \sum_{i=1}^{n} ([X_i] - [\hat{X}_i])^2 \qquad (3)$$

241 where $[X_i]$ and $[\hat{X}_i]$ are respectively experimental and predicted concentrations of X, and n
242 is the number of experimental points.

243 The coefficient of determination R^2 was calculated from the ratio of the explained variance to
244 the total variance (TSS), with the explained variance being TSS minus RSS:

245 $$R^2 = \frac{\sum_{i=1}^{n} ([X_i] - [\overline{X}])^2 - RSS}{\sum_{i=1}^{n} ([X_i] - [\overline{X}])^2}$$

246 where $[\overline{X}]$ is the mean concentration of X, and n is the number of experimental points.

247 For multi-response models, RSS was also used to calculate the Akaike information criterion
248 (AIC). AIC is a complementary measure of goodness of fit that was used by van Boekel
249 (2008) [30] and which describes the trade-off between the model accuracy (RSS) and
250 complexity, i.e. the number of parameters (equation 4).

251 $$AIC = n \ln\left(\frac{RSS}{n}\right) + 2(p+1) \qquad (4)$$

Where *n* is the data number and *p* is the number of estimated parameters. AIC is an interesting criterion because it enables comparison of models having a different number of parameters. A small AIC indicates that the model presents a suitable goodness of fit to the experimental data while having a limited number of parameters.

Kinetic parameter uncertainty

Parameter uncertainty of the optimized parameters obtained with the Levenberg-Marquardt algorithm was calculated by non-linear error propagation using Matlab® software (Mathworks Inc., Natick, Mass, USA).

Results and discussion

Identification of carotenoids from fresh and heated grapefruit juice

The two major carotenoids found in fresh grapefruit juice (*Citrus paradise* Macf) were all-*trans*-β-carotene and all-*trans*-lycopene, at 1.25 ± 0.14 and 5.78 ± 0.58 mg L^{-1}, respectively, with the latter representing 80% of both (Fig 1A). The order of magnitude of the ratio lycopene/β-carotene found was close to that of the three found by Xu *et al.* (2006) in red grapefruit [6]. In heated grapefruit juice, β-carotene and lycopene isomerization was observed (Fig 1B). Thermal treatment led to a significant increase in 13-*cis*-β-carotene and 9-*cis*-β-carotene. Heating also increased lycopene isomers, i.e. three *cis* isomers were tentatively identified, namely 5-*cis*, 9-*cis* and 13-*cis*-lycopene, according to their *cis*-peak intensity and maximal absorption wavelength [18, 19, 31]. For 13-*cis*-lycopene, the *cis*-peak intensity, expressed as $\%_{AB/AII}$, was higher compared to that of 9-*cis*-lycopene because the *cis* double bond is closer to the centre of the molecule. A hypsochromic shift of 6 nm occurred when *cis* was compared to the all-*trans*-compound and this trend was similar to that reported in the literature [24, 27, 31].

277

278 **Carotene degradation kinetics in real juice and model media during thermal treatment**

279 Kinetic models were drawn up on the basis of the analysis of experimental concentrations
280 over the thermal treatment time for each carotene, i.e. β-carotene and lycopene. By
281 incrementing α, the apparent order of the reaction in Eq. 1 and the calculation of the
282 corresponding RSS (Eq. 3), second-order kinetics appeared to best fit the experimental data
283 (minimal RSS). Most previously reported studies uses first-order kinetics to model carotene
284 loss [12]. However, other orders have also been reported, especially in non-aqueous solvents [32,
285 33]. Recently, Colle (2010) used a fractional conversion model to represent lycopene
286 degradation in an olive oil/tomato emulsion. Indeed, they found that the carotene degradation
287 pattern was that of an equilibrated reaction (non-zero plateau), which was also observed in
288 real juice in our study [31]. However, a second-order kinetic model was preferred to compare all
289 rate constants (in real juice and ethanol/water mixture).

290 The resulting rate constants and activation energies are presented in Table 1. All rate
291 constants increased with temperature. The rate constants of β-carotene and lycopene were
292 generally close. In similar matrixes and temperature conditions, their degradation rate was 2-
293 to 10-fold lower than that of hydroxy-carotenoids (xanthophylls) [34]. Therefore carotenes are
294 more stable because of the absence of hydroxyl groups. However, despite this structural
295 similarity, their rate constants of the two carotenes varied differently as a function of the
296 matrix. For instance, in real juice, the β-carotene rate constants ($8.83 \cdot 10^{-3} \pm 1.03 \cdot 10^{-3}$ to
297 $5.14 \cdot 10^{-2} \pm 2.17 \cdot 10^{-2}$ kg^{-1} m^3 s^{-1}) were 3- to 80-fold superior to the values obtained for
298 lycopene, in accordance with the findings of Abushita *et al.* (2000), D'Evoli *et al.* (2013) and
299 Chanforan *et al.* (2012). Indeed, they all found greater stability of lycopene compared to β-
300 carotene in a vegetable matrix during heat treatment (tomato). They explained this difference
301 in behaviour by the fact that lycopene was more stable when bound to protein inside the

vegetable matrix. However, when lycopene was not protein-bound, they showed that this pigment was less stable than β-carotene [18, 35, 36]. This is interesting because we also noted an inversion of stability when carotenes were not in their initial matrix. Indeed, in all acid media (AM, AM+AA, AM+NAR), the reaction rates of lycopene at 90 and 95°C were 1.2- to 3.6-fold higher than those of β-carotene. β-carotene was also less stable out of its original matrix, but to a lesser extent. In comparison to real grapefruit juice, the lycopene rate constant increased from 1- to 14-fold as a function of the temperature in the acid medium (AM), while it increased from 1- to 2-fold for β-carotene.

The activation energy of 45±10 kJ.mol^{-1} for β-carotene in grapefruit juice was in accordance with that found by Colle *et al.* (2013) in tomato emulsion (45 kJ mol^{-1}) but lower than that reported by Dhuique-Mayer *et al.* (2007) in orange juice (110 kJ mol^{-1}) [14, 24]. The activation energy of lycopene was 26±10 kJ mol^{-1} in real juice. Lycopene was thus more sensitive to an increase of temperature than β-carotene, with an activation energy close to that reported for tomato pulp and watermelon juice (19.5 and 26.4 kJ mol^{-1}) [22, 23].

Very few studies have compared the activation energies of lycopene and β-carotene in the same vegetal matrix. Demiray *et al.* (2013) found activation energies of 47 and 40 kJ.mol^{-1} for lycopene and β-carotene, respectively, in tomato quarters during drying [37]. Colle *et al.* (2013) found activation energies of 28 and 45 kJ.mol^{-1} for lycopene and β-carotene, respectively, in tomato emulsion during thermal treatment, which is out of line with the findings of Demiray *et al.* (2013)[24, 37]. Activation energies should therefore be considered very carefully because they highly depend on the matrix and temperature field studied [12].

When carotenes were out of their matrix (i.e. in AM), the activation energies did not substantially change for β-carotene but increased from 26±10 to 89±23 kJ.mol^{-1} for lycopene. The marked increase in the activation energy of lycopene (70%) showed that this carotene was particularly vulnerable and sensitive to an increase of temperature when isolated from the

matrix. Therefore, the juice matrix impacted both the rate constants and activation energies and had a protective role for carotenes, and especially lycopene. This was also demonstrated for xanthophylls in a previous study [34]. This protective role could have structural (by covalent or weak bonds or different matter state) or chemical origins. This latter hypothesis was tested by the addition to the acid medium of ascorbic acid (AM+AA) or naringin (AM+NAR), which are major phytochemicals of citrus juice that could have a protective effect. Regarding the rate constants, the addition of ascorbic acid did not significantly change the degradation trends from 75 to 95°C for β-carotene and lycopene. Indeed, the degradation rate constant of β-carotene was $6.14 \cdot 10^{-2} \pm 1.03 \cdot 10^{-2}$ at 90°C in AM+AA compared to $6.72 \cdot 10^{-2} \pm 1.27 \cdot 10^{-2}$ kg^{-1} m^3 s^{-1} in AM alone. Moreover, for lycopene, the degradation rate constant in the same conditions was $7.17 \cdot 10^{-2} \pm 2.52 \cdot 10^{-2}$ in AM+AA and $9.23 \cdot 10^{-2} \pm 2.03 \cdot 10^{-2}$ kg^{-1} m^3 s^{-1} in AM alone. Conversely, at 60°C in AM+AA, the degradation rate was 5-fold higher for β-carotene and 17-fold higher for lycopene. This in turn decreased the activation energy from 40±10 to 19±6 kJ mol^{-1} for β-carotene and more slightly from 89±23 to 79±20 kJ mol^{-1} for lycopene. The interaction between ascorbic acid and carotenes is questioned and not well documented. Indeed, these molecules that have different polarity are supposed to interact at the interfaces in food matrices. Results reported by Sanchez et al. (2002) showed that vitamin C could preserve carotenoid compounds from oxidation in orange juice, but no mechanism was explained [38]. In contrast, Kanner *et al.* (1977) showed that ascorbic acid could have pro-oxidant effects with metal salts toward β-carotene in a linoleate system [39]. In an ethanol/water mixture, ascorbic acid and carotenes may interact as well. This interaction is only visible at 60°C but no longer at 75°C and higher temperatures. This may be partly explained by the thermolability of ascorbic acid in acid medium (AM+AA). Indeed, while 60% of ascorbic acid was retained at 300 min-60°C, degradation was almost total after 300 min-95°C. However, according to the study of Dhuique-Mayer *et al.* (2007), the retention of ascorbic

acid after 150 min at 100°C was 55% in citrus juice [14]. This therefore suggests that there was substantial retention of vitamin C throughout more than the half of the experiment conducted at 95°C. Other explanation of this weak impact of ascorbic acid at high temperature could be the decrease in the dissolved oxygen concentration, which is known to be involved in ascorbic acid oxidation reactions. The influence of ascorbic acid on the carotenoid degradation rate therefore decreases as the temperature increases. The addition of naringin impacted the rate constants but only at high temperatures. For β-carotene, the rate constants were slightly lower until 75°C but 2-fold higher at 95°C. This resulted in a strong 40±10 to 138±15 $kJ.mol^{-1}$ increase in activation energy. At moderate temperature (60°C), the result was in accordance with a previous study that highlighted the protective effect of polyphenols on β-carotene at ambient temperature [40]. However, this protective role was not observed at higher temperature, and the addition of naringin even seemed to increase β-carotene degradation. For lycopene, the rate constants were on average 3-fold higher in AM+NAR. It is noteworthy that naringin is thermostable [41] (no significant degradation observed). Interactions between polyphenols and carotene at different temperatures therefore need to be elucidated.

Rate constants and activation energies were higher in all model systems than in juice, especially for lycopene. The addition of ascorbic acid and naringin did not show a substantial improvement in stability in model systems. Indeed, ascorbic acid had no influence beyond 75°C, while naringin seemed to increase its degradation from 75°C. The protective effect of the juice matrix revealed in these experiments thus more have been due to structural protection than to phytochemicals. Indeed, in plant tissues, especially in citrus pulp, carotenoids are localized in chromoplasts within pulp particles. The particle sizes of citrus pulp are from 1 μm to 1 mm in juices [42]. During processing, carotenoids may be released from the matrix and undergo degradation because of the interaction with other fruit constituents (ascorbic acid, flavonoids, etc.). Therefore the degradation rate is partly controlled by mass

transfer from the pulp to the liquid fraction. In the model systems used in this study, carotenoids were homogenously dispersed in a water/ethanol mixture with particles that were assumed to be very small due to this type of spontaneous micro-emulsion. Carotenoid degradation was thus less delayed by mass transfer and surface contact was enhanced because of the emulsion. Despite these differences, the model systems were very convenient as they enabled composition control and, even though they did not mimic the real juice exactly, the carotenoid reactivity did not differ markedly when comparing rate constants in PJ and AM, especially for β-carotene. The conclusions drawn in model systems concerning the interaction with micro-constituents could therefore be transferable to real matrices. Besides this model system approach, the role of structures surrounding carotenoids in the vegetable matrix, even destructured (juice), should to be specified with further works based on microscopic observations, especially for lycopene**.**

Multi-response modelling of carotene thermal degradation in model media

β-carotene and lycopene degradation was limited in real juice (low rate constant), but it was significant in model media. In addition, high amounts of isomers could be measured in such media (dots in Fig. 3 and 4). After 100 min-95°C, *cis*-isomers could proportionally represent 40% and 60 % of total β-carotene and lycopene, respectively. The amount of other degradation compounds–which were assumed to be oxidation and cleavage compounds (OCC)–was assessed at each time via mass balance calculation. From these data, we could represent both β-carotene degradation and the formation of neoformed isomers and other degradation compounds according the different reaction schemes proposed in Fig. 2, from the simplest (hypothesis 1) to the most complex (hypothesis 4). The four hypotheses represent different possibilities for carotenoid degradation. Isomer formation before oxidation and cleavage has been documented in many studies about carotenoids [12]. Hypothesis 1 is the

simplest two-step reaction. Hypothesis 2 involves a reverse isomerization reaction which was also assumed to occur in previous studies [27]. Hypothesis 3 and 4 are the same as hypothesis 1 and 2, with the addition of direct cleavage from *trans*-carotenoids. Kinetic quantification of this direct reaction may provide evidence of the prevalence of oxidation reactions. Each hypothesis was transformed into an ordinary differential equation system including the different rate constants. As these schemes tend to describe each reaction step, the order for every reaction was assumed to be one. A multi-response modelling procedure enabled the identification of individual rate constants and the generation of modelled data (lines in Figs. 3 and 4). The best hypothesis of Fig. 2 was chosen by calculating the discrepancy between the experimental and simulated data (RSS) and the AIC criterion expressing the best trade-off between accuracy and complexity. For β-carotene, substantial lower RSS and AIC were found for hypothesis 4. Therefore, rate constants k_{ci}, k_{co} were the degradation constants of β-carotene in isomers and other oxidative and cleavage compounds (OCC), respectively.

Isomer rate constants were k_{ic} and k_{io} for retroisomerization in the *trans* form or the degradation in OCC, respectively. β-carotene retroisomerization was also demonstrated in oil medium by Achir *et al.* (2011)[27]. All rates were identified at each temperature. The k_{ref} extracted from eq. 2 at a reference temperature of 80°C are presented in Table 2. AA and NAR increased the k_{ci} isomerization constant from 3- to 7-fold, respectively. The k_{ic} retroisomerization constant only increased by 6.5-fold in the case of AA, while it decreased slightly with NAR. The k_{ci}/k_{ic} isomerization equilibrium constant could thus be calculated: 0.53 for AM, 0.32 for AM+AA, and 7 for AM+NAR. In the case of NAR, the equilibrium constant was thus higher, thus highlighting the importance of isomerization reactions. k_{co} increased by a 4-fold with AA addition. Direct β-carotene oxidation was thus promoted with this molecule. In contrast, k_{co} was very low with NAR, while k_{io} was 3-fold higher ($2.60\ 10^{-5} \pm 1.3\ 10^{-5}$ instead of $7.67\ 10^{-6} \pm 1.5\ 10^{-6}\ s^{-1}$). Hence, with the addition of NAR, β-carotene was

427 strongly isomerized and the formed isomers were very sensitive to oxidation and cleavage,
428 giving rise to OCC.
429 In the case of lycopene, hypothesis 3 was sufficient to represent the experimental data (lowest
430 RSS and AIC). The mechanisms therefore seemed to be different: no retroisomerization was
431 identified with this approach. In this case, k_{ci} was the isomerization constant, k_{co} the direct
432 oxidation constant and k_{io} the isomer oxidation. With the addition of AA, k_{ci} and k_{io} remained
433 the same. The only difference was the 3-fold increase in k_{co}, which was the direct oxidation
434 rate. This confirmed that AA enhanced direct oxidation. With the addition of NAR, k_{ci} et k_{io}
435 decreased by 27- and 70-fold, while k_{co} increase by 4-fold. Regarding lycopene, direct
436 oxidation of this compound was also enhanced by NAR. Hence, designing a model system
437 associated with multi-response modelling may be useful to predict neoformation of
438 compounds such as isomers during thermal processes, but it is also a way to quantify the
439 kinetic importance of each reaction path as a function of the formulation, and therefore gain
440 insight into the micro-consituent reaction mode. Further studies are now needed to better
441 understand the interactions between carotenoids, polyphenols and ascorbic acid, which are
442 very important phytochemicals in juice from nutritional and organoleptic standpoints.
443

444

445 **References**

446 1. Uckoo, R. M.; Jayaprakasha, G. K.; Balasubramaniam, V. M.; Patil, B. S., Grapefruit
447 (Citrus paradisi Macfad) phytochemicals composition is modulated by household processing
448 techniques. *J. Food Sci.* **2012**, *77*, 921-926.
449 2. Tanaka, T.; Tanaka, T.; Tanaka, M.; Kuno, T., Cancer Chemoprevention by Citrus
450 Pulp and Juices Containing High Amounts of β-Cryptoxanthin and Hesperidin. *J. Biomed.*
451 *Biotechnol.* **2012**, doi: 10.1155/2012/516981.
452 3. Gorinstein, S.; Caspi, A.; Libman, I.; Tzvi Lerner, H.; Huang, D.; Leontowicz, H.;
453 Leontowicz, M.; Tashma, Z.; Katrich, E.; Shengbao, F.; Trakhtenberg, S., Red Grapefruit
454 Positively Influences Serum Triglyceride Level in Patients Suffering from Coronary
455 Atherosclerosis: Studies in Vitro and in Humans. *J. Agric. Food Chem.* **2006**, *54*, 1887-
456 1892.
457 4. Gorinstein, S.; Leontowicz, H.; Leontowicz, M.; Krzeminski, R.; Gralak, M.;
458 Delgado-Licon, E.; Martinez Ayala, A. L.; Katrich, E.; Trakhtenberg, S., Changes in plasma
459 lipid and antioxidant activity in rats as a result of naringin and red grapefruit supplementation.
460 . *J. Agric. Food Chem.* **2005**, *53*, 3223-3228.
461 5. Poulaert, M.; Borel, P.; Caporiccio, B.; Gunata, Z.; Dhuique-Mayer, C., Grapefruit
462 juices impair the bioaccessibility of β-carotene from orange-fleshed sweet potato but not its
463 intestinal uptake by Caco-2 cells. *J. Agric. Food Chem.* **2012**, *60*, 685-691.
464 6. Xu, J.; Tao, N.; Liu, Q.; Deng, X., Presence of diverse ratios of lycopene/β-carotene in
465 five pink or red-fleshed citrus cultivars. *Sci. Hortic.* **2006**, *108*, 181-184.
466 7. Honest, K. N.; Zhang, H. W.; Zhang, L. F., Lycopene: Isomerization Effects on
467 Bioavailability and Bioactivity Properties. *Food Rev. Int.* **2011**, *27*, 248-258.

8. Hiranvarachat, B.; Suvarnakuta, P.; Devahastin, S., Isomerisation kinetics and antioxidant activities of [beta]-carotene in carrots undergoing different drying techniques and conditions. *Food Chem.* **2008**, *107*, 1538-1546.

9. Marx, M.; Stuparic, M.; Schieber, A.; Carle, R., Effects of thermal processing on trans-cis-isomerization of β-carotene in carrot juices and carotene-containing preparations. *Food Chem.* **2003**, *83*, 609-617.

10. Rodriguez, E. B.; Rodriguez-Amaya, D. B., Formation of apocarotenals and epoxycarotenoids from [beta]-carotene by chemical reactions and by autoxidation in model systems and processed foods. *Food Chem.* **2007**, *101*, 563-572.

11. Bechoff, A.; Dhuique-Mayer, C.; Dornier, M.; Tomlins, K. I.; Boulanger, R.; Dufour, D.; Westby, A., Relationship between the kinetics of [beta]-carotene degradation and formation of norisoprenoids in the storage of dried sweet potato chips. *Food Chem.* **2010**, *121*, 348-357.

12. Penicaud, C.; Achir, N.; Dhuique-Mayer, C.; Dornier, M.; Bohuon, P., Degradation of β-carotene during fruits and vegetables processing or storage: reaction mechanisms and kinetics aspects. *Fruits* **2011**, *66*, 417-440.

13. Vikram, V. B.; Ramesh, M. N.; Prapulla, S. G., Thermal degradation kinetics of nutrients in orange juice heated by electromagnetic and conventional methods. *J. Food Eng.* **2005**, *69*, 31-40.

14. Dhuique-Mayer, C.; Tbatou, M.; Carail, M.; Caris-Veyrat, C.; Dornier, M.; Amiot, M. J., Thermal Degradation of Antioxidant Micronutrients in Citrus Juice: Kinetics and Newly Formed Compounds. *J. Agric. Food Chem.* **2007**, *55*, 4209-4216.

15. Ahmed, J.; Shivhare, U. S.; Sandhu, K. S., Thermal Degradation Kinetics of Carotenoids and Visual Color of Papaya Puree. *J. Food Sci.* **2002**, *Volume 67*, 2692 - 2695.

16. Lee, M. T.; Chen, B. H., Stability of lycopene during heating and illumination in a model system. *Food Chem.* **2002**, *78*, 425–432.

17. Schierle, J.; Bretzel, W.; Buhler, I.; Faccin, N.; Hess, D.; Steiner, K.; Schuep, W., Content and isomeric ratio of lycopene in food and human blood plasma. *Food Chem.* **1997**, *59*, 459–465.

18. Chanforan, C. l.; Loonis, M. l.; Mora, N.; Caris-Veyrat, C.; Dufour, C., The impact of industrial processing on health-beneficial tomato microconstituents. *Food Chem.* **2012**, *134*, 1786-1795.

19. Xu, Y.; Pan, S., Effects of various factors of ultrasonic treatment on the extraction yield of all-trans-lycopene from red grapefruit (Citrus paradise Macf.). *Ultrason Sonochem* **2013**, *20*, 1026-1032.

20. Lee, M. T.; Chen, B. H., Stability of lycopene during heating and illumination in a model system. *Food Chem.* **2002**, *78*, 425-432.

21. Huawei, Z.; Xiaowen, W.; Elshareif, O.; Hong, L.; Qingrui, S.; Lianfu, Z., Isomerisation and degradation of lycopene during heat processing in simulated food system. *Int. Food Res. J.* **2014**, *21*, 45.

22. Goula, A. M.; Adamopoulos, K. G.; Chatzitakis, P. C.; Nikas, V. A., Prediction of lycopene degradation during a drying process of tomato pulp. *J. Food Eng.* **2006**, *74*, 37-46.

23. Sharma, R.; Kaur, D.; Oberoi, D. P. S.; Sogi, D. S., Thermal degradation kinetics of pigments and visual color in watermelon juice. *Int. J. Food Prop.* **2008**, *11*, 439-449.

24. Colle, I. J. P.; Lemmens, L.; Van Buggenhout, S.; Van Loey, A. M.; Hendrickx, M. E., Modeling Lycopene Degradation and Isomerization in the Presence of Lipids. *Food Bioprocess Technol.* **2013**, *6*, 909-918.

515 25. Zepka, L. Q.; Borsarelli, C. D.; Azevedo, M. A.; da Silva, P.; Mercadante, A. Z.,
516 Thermal Degradation Kinetics of Carotenoids in a Cashew Apple Juice Model and Its Impact
517 on the System Color. *J. Agric. Food Chem.* **2009**, *57*, 7841-7845.
518 26. Zepka, L. Q.; Mercadante, A. Z., Degradation compounds of carotenoids formed
519 during heating of a simulated cashew apple juice. *Food Chem.* **2009**, *117*, 28-34.
520 27. Achir, N.; Pénicaud, C.; Avallone, S.; Bohuon, P., Insight into β-carotene thermal
521 degradation in oils with multiresponse modelling. *J. Am. Oil Chem. Soc.* **2011**, *88*, 2035-
522 2045.
523 28. Achir, N.; Pénicaud, C.; Bechoff, A.; Boulanger, R.; Dornier, M.; Dhuique-Mayer, C.,
524 Use of Multi-response Modelling to Investigate Mechanisms of β-Carotene Degradation in
525 Dried Orange-Fleshed Sweet Potato During Storage: from Carotenoids to Aroma Compounds.
526 *Food Bioprocess Technol.* **2014**, *7*, 1656-1669
527 29. Dhuique-Mayer, C.; Caris-Veyrat, C.; Ollitrault, P.; Curk, F.; Amiot, M. J., Varietal
528 and Interspecific Influence on Micronutrient Contents in Citrus from the Mediterranean Area.
529 *J. Agric. Food Chem.* **2005**, *53*, 2140-2145.
530 30. van Boekel, M. A. J. S., *Kinetic Modeling of Reactions in Foods*. CRC Press: 2008.
531 31. Colle, I.; Lemmens, L.; Tolesa, G.; Van Buggenhout, S.; De Vleeschouwer, K.; Van
532 Loey, A.; Hendrickx, M., Lycopene degradation and isomerization kinetics during thermal
533 processing of an olive oil/tomato emulsion. *J. Agric. Food Chem.* **2010**, *58*, 12784-12789.
534 32. Shin, J. H.; Chung, H. L.; Seo, J. K.; Sim, J. H.; Huh, C. S.; Kil, S. K.; Baek, Y. J.,
535 Degradation Kinetics of Capsanthin in Paprika (Capsanthin annuum L.) as Affected by
536 Heating. *J. Food Sci.* **2001**, *66*, 15-18.
537 33. Achir, N.; Randrianatoandro, V. A.; Bohuon, P.; Laffargue, A.; Avallone, S., Kinetic
538 study of beta-carotene and lutein degradation in oils during heat treatment. *Eur. J. Lipid*
539 *Sci. Technol.* **2010**, *112,* 349-361.

34. Hadjal, T.; Dhuique-Mayer, C.; Madani, K.; Dornier, M.; Achir, N., Thermal degradation kinetics of xanthophylls from blood orange in model and real food systems. *Food Chem.* **2013**, *138*, 2442-2450.

35. Abushita, A. A.; Daood, H. G.; Biacs, P. A., Change in carotenoids and antioxidant vitamins in tomato as a function of varietal and technological factors. *J. Agric. Food Chem.* **2000**, *48*, 2075-2081.

36. D'Evoli, L.; Lombardi-Boccia, G.; Lucarini, M., Influence of Heat Treatments on Carotenoid Content of Cherry Tomatoes. *Foods* **2013**, *2*, 352-363.

37. Demiray, E.; Tulek, Y.; Yilmaz, Y., Degradation kinetics of lycopene, β-carotene and ascorbic acid in tomatoes during hot air drying. *LWT-Food Sci. Technol.* **2013**, *50*, 172-176.

38. Sanchez-Moreno, C.; Plaza, L.; de Ancos, B.; Cano, M. P., Vitamin C, Provitamin A Carotenoids, and Other Carotenoids in High-Pressurized Orange Juice during Refrigerated Storage. *J. Agric. Food Chem.* **2002**, *51*, 647-653.

39. Kanner, J.; Mendel, H.; Budomski, P., Prooxidant and antioxidant effects of ascorbic acid and metal salts in a β-carotene-linoleate model system. *J. Food Sci.* **1977**, *42*, 60-64. .

40. Unten, L.; Koketsu, M.; Kim, M., Antidiscoloring activity of green tea polyphenols on beta-carotene. *J. Agric. Food Chem.* **1997**, *45*, 2009–2012.

41. Yuan, Q.; Yao, X. L.; Feng, G.; Huang, Q., Characteristic changes of naringin in grapefruit juice during heat treatment. *Food Sci. Technol.* **2012**, *7*.

42. Buslig, B. S.; Carter, R. D., Particle size distribution in orange juices. *Fla. State Hortic. Soc.* **1974**, 302-305.

563 **Figure captions**

564

565 Fig. 1. HPLC chromatogram: A) in fresh pink grapefruit juice peaks 1 (β-carotene) and 2
566 (lycopene), and B) in heated grapefruit juice for 5 h at 95°C (peaks 3, 4: β-carotene isomers;
567 peaks 5,6,7: lycopene isomers).

568 Fig. 2. Presumed model of thermal degradation of lycopene, β-carotene (all-*trans*) and of their
569 isomers in model systems.

570 Fig. 3. Experimental concentrations in mg L^{-1} over time during heat treatments at four
571 temperatures (dots: ♦ 60 • 75 ▲ 95 ■ 95 °C) of β-carotene, isomers and other degradation
572 products (OCC) in: A) citrate buffer/ethanol mixture (AM), B) with added ascorbic acid
573 (AM+AA), and C) with added naringin (AM+NAR). Error bars represent the standard
574 deviation (n = 3) and lines represent the modelled data.

575 Fig. 4. Experimental concentrations in mg L^{-1} over time during heat treatments at four
576 temperatures (dots: ♦ 60 • 75 ▲ 95 ■ 95 °C) of lycopene, isomers and other degradation
577 products (OCC) in: A) citrate buffer/ethanol mixture (AM), B) with added ascorbic acid
578 (AM+AA), and C) with added naringin (AM+NAR). Error bars represent the standard
579 deviation (n = 3) and lines represent the modelled data.

580

581 Table 1. Second-order rate constants in kg^{-1} m^3 s^{-1} and Arrhenius parameters, reference
582 constant in kg^{-1} m^3 s^{-1} at 80°C and activation energies in kJ mol^{-1} of all-*trans*-β-carotene and
583 all-*trans*-lycopene loss in real juice and model media.

584 Table 2. Rate constants of lycopene and β-carotene thermal degradation from multi-response
585 modelling in model media at the reference temperature (80°C) according to hypotheses 3 and
586 4, respectively (Fig 2).

Table 1

Medium	$k_{60\,°C}$	$k_{75\,°C}$	$k_{90\,°C}$	$k_{95\,°C}$	k_{ref}	Ea	R^2
	All-trans-β-carotene						
Real juice	$8.83\ 10^{-3}$ ($1.03\ 10^{-3}$)	$2.35\ 10^{-2}$ ($4.81\ 10^{-3}$)	$5.62\ 10^{-2}$ ($2.99\ 10^{-2}$)	$5.14\ 10^{-2}$ ($2.17\ 10^{-2}$)	$3.08\ 10^{-2}$ ($5.37\ 10^{-3}$)	45 (10)	0.97
AM	$5.26\ 10^{-3}$ ($2.32\ 10^{-3}$)	$4.89\ 10^{-2}$ ($1.46\ 10^{-2}$)	$6.72\ 10^{-2}$ ($1.27\ 10^{-2}$)	$7.25\ 10^{-2}$ ($2.27\ 10^{-2}$)	$4.42\ 10^{-2}$ ($7.17\ 10^{-3}$)	40 (10)	0.87
AM+AA	$2.42\ 10^{-2}$ ($3.93\ 10^{-3}$)	$5.44\ 10^{-2}$ ($3.38\ 10^{-3}$)	$6.14\ 10^{-2}$ ($1.03\ 10^{-3}$)	$5.77\ 10^{-2}$ ($1.03\ 10^{-3}$)	$4.85\ 10^{-3}$ ($5.56\ 10^{-2}$)	19 (6)	0.80
AM+NAR	$3.59\ 10^{-3}$ ($1.79\ 10^{-4}$)	$1.71\ 10^{-2}$ ($3.32\ 10^{-3}$)	$8.63\ 10^{-2}$ ($1.52\ 10^{-2}$)	$1.68\ 10^{-1}$ ($3.03\ 10^{-2}$)	$2.42\ 10^{-2}$ ($4.82\ 10^{-3}$)	138 (15)	0.99
	All-trans-lycopene						
Real juice	$1.02\ 10^{-4}$ ($2.73\ 10^{-5}$)	$9.04\ 10^{-3}$ ($4.10\ 10^{-3}$)	$8.76\ 10^{-3}$ (4 $32\ 10^{-3}$)	$7.00\ 10^{-3}$ ($3.21\ 10^{-3}$)	$6.08\ 10^{-3}$ ($2.11\ 10^{-3}$)	26 (10)	0.68
AM	$8.90\ 10^{-4}$ ($1.03\ 10^{-4}$)	$1.65\ 10^{-2}$ ($3.83\ 10^{-3}$)	$9.23\ 10^{-2}$ ($2.03\ 10^{-2}$)	$1.04\ 10^{-1}$ ($2.02\ 10^{-2}$)	$3.25\ 10^{-2}$ ($1.37\ 10^{-3}$)	89 (23)	0.99
AM+AA	$1.48\ 10^{-2}$ ($2.52\ 10^{-3}$)	$1.07\ 10^{-2}$ ($6.36\ 10^{-3}$)	$7.17\ 10^{-2}$ ($2.52\ 10^{-2}$)	$8.86\ 10^{-2}$ ($1.12\ 10^{-2}$)	$3.06\ 10^{-2}$ ($8.96\ 10^{-3}$)	79 (20)	0.67
AM+NAR	$3.21\ 10^{-3}$ ($5.05\ 10^{-4}$)	$3.47\ 10^{-2}$ ($1.77\ 10^{-3}$)	$2.92\ 10^{-1}$ ($3.15\ 10^{-2}$)	$2.89\ 10^{-1}$ ($4.84\ 10^{-2}$)	$1.08\ 10^{-1}$ ($4.91\ 10^{-3}$)	79 (23)	0.98

AM: citrate buffer/ethanol mixture

AM+AA: citrate buffer/ethanol mixture with added ascorbic acid

AM+NAR: citrate buffer/ethanol mixture with added naringin

Table 2

β-carotene rate constants k_{ref} (s^{-1}) of hypothesis 4 at 80°C reference temperature				Lycopene rate constants k_{ref} (s^{-1}) of hypothesis 3 at 80°C reference temperature			
	AM	AM+AA	AM+NAR		AM	AM+AA	AM+NAR
k_{ci}	$2.40\ 10^{-5}$ ($6.3\ 10^{-6}$)	$9.03\ 10^{-5}$ ($1.2\ 10^{-5}$)	$1.53\ 10^{-4}$ ($2.2\ 10^{-5}$)	k_{ci}	$4.88\ 10^{-5}$ ($5.0\ 10^{-6}$)	$3.25\ 10^{-5}$ ($6.3\ 10^{-6}$)	$1.75\ 10^{-6}$ ($8.6\ 10^{-7}$)
k_{co}	$1.18\ 10^{-5}$ ($3.4\ 10^{-6}$)	$4.30\ 10^{-5}$ ($2.2\ 10^{-6}$)	$6.09\ 10^{-8}$ ($2.3\ 10^{-8}$)	k_{co}	$1.05\ 10^{-5}$ ($2.5\ 10^{-6}$)	$3.02\ 10^{-5}$ ($1.2\ 10^{-5}$)	$4.17\ 10^{-5}$ ($5.4\ 10^{-6}$)
k_{ic}	$4.48\ 10^{-5}$ ($2.4\ 10^{-5}$)	$2.95\ 10^{-4}$ ($6.5\ 10^{-5}$)	$2.30\ 10^{-5}$ ($1.0\ 10^{-5}$)				
k_{io}	$7.67\ 10^{-6}$ ($1.5\ 10^{-6}$)	$4.66\ 10^{-7}$ ($9.2\ 10^{-8}$)	$2.60\ 10^{-5}$ ($1.3\ 10^{-5}$)	k_{io}	$1.68\ 10^{-4}$ ($5.3\ 10^{-5}$)	$1.75\ 10^{-4}$ ($6.3\ 10^{-5}$)	$2.39\ 10^{-6}$ ($1.3\ 10^{-6}$)
RSS	0.88	2.78	2.73		7.19	3.57	4.07
R^2	0.95	0.90	0.96		0.92	0.65	0.98

AM: citrate buffer/ethanol mixture

AM+AA: citrate buffer/ethanol mixture with added ascorbic acid

AM+NAR: citrate buffer/ethanol mixture with added naringin

Figure 1

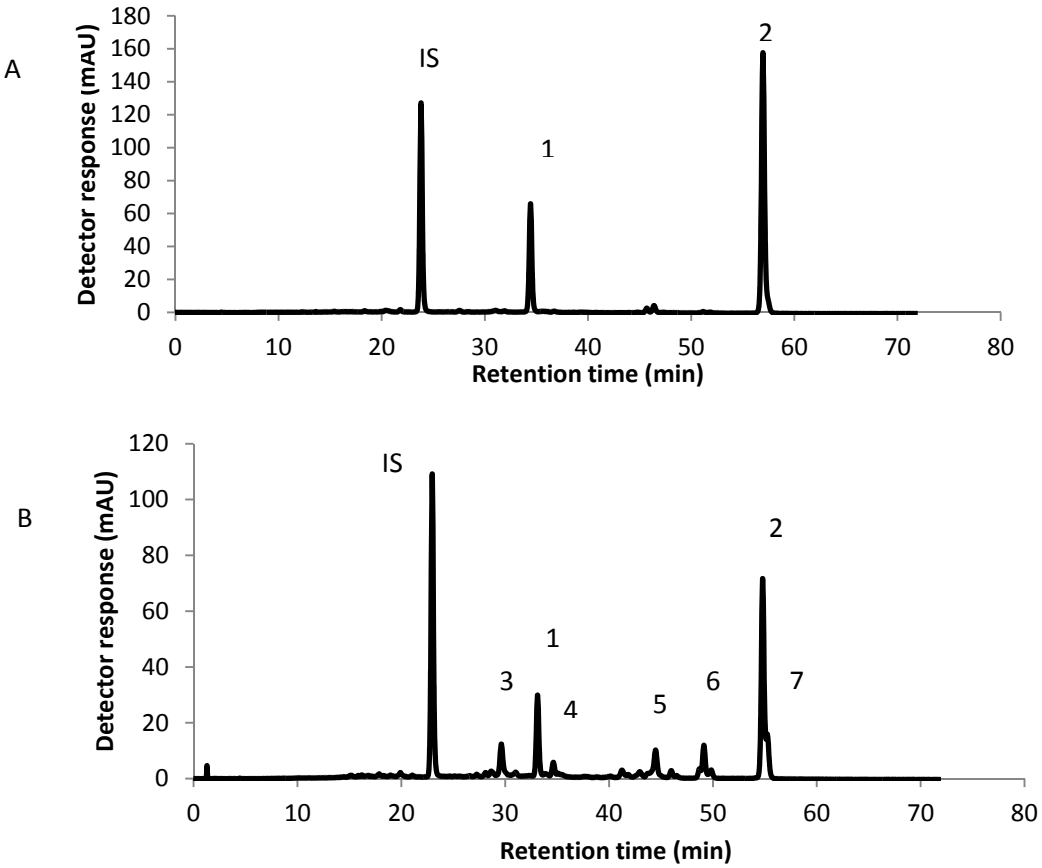

IS: Internal standard

Figure 2

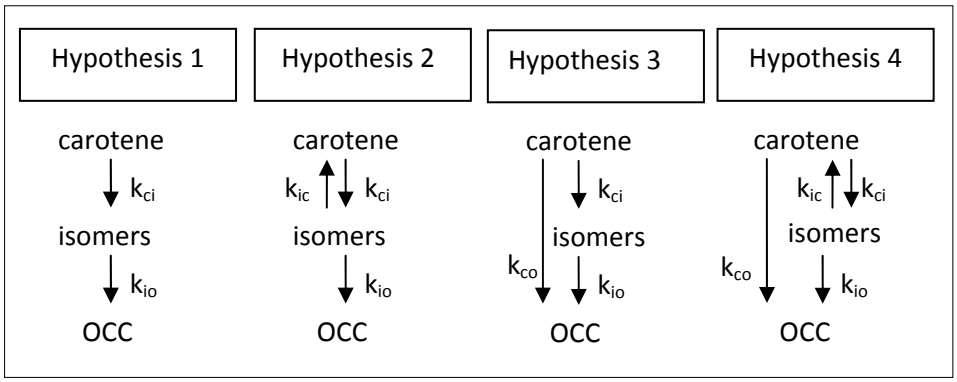

OCC : Oxidation and Cleavage Compounds
k_{ci}: rate constant of isomerisation
k_{io}: rate constant of oxidation via isomer
k_{co}: rate constant of direct oxidation
k_{ic}: rate constant of retroisomerisation

Figure 3

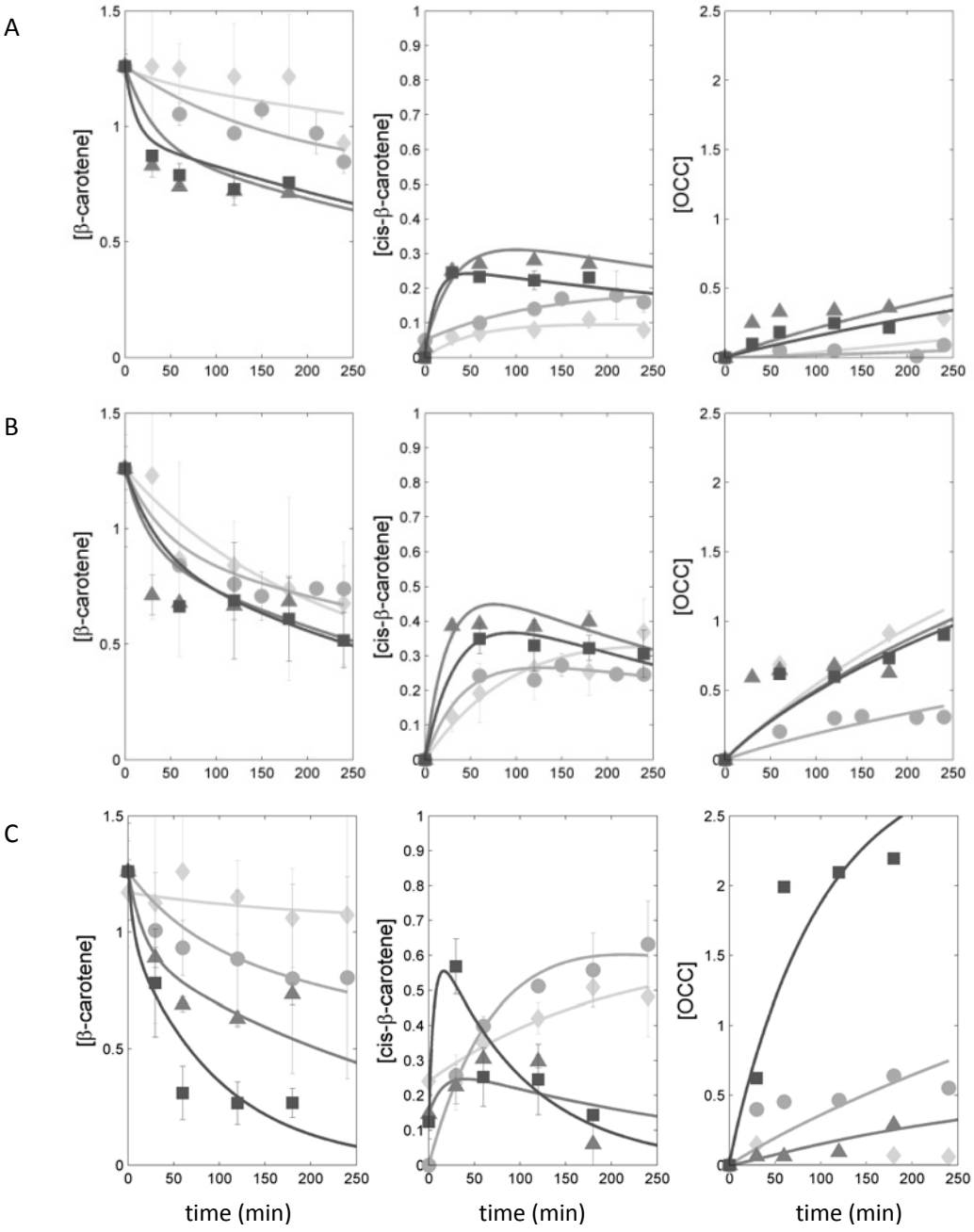

Figure 4

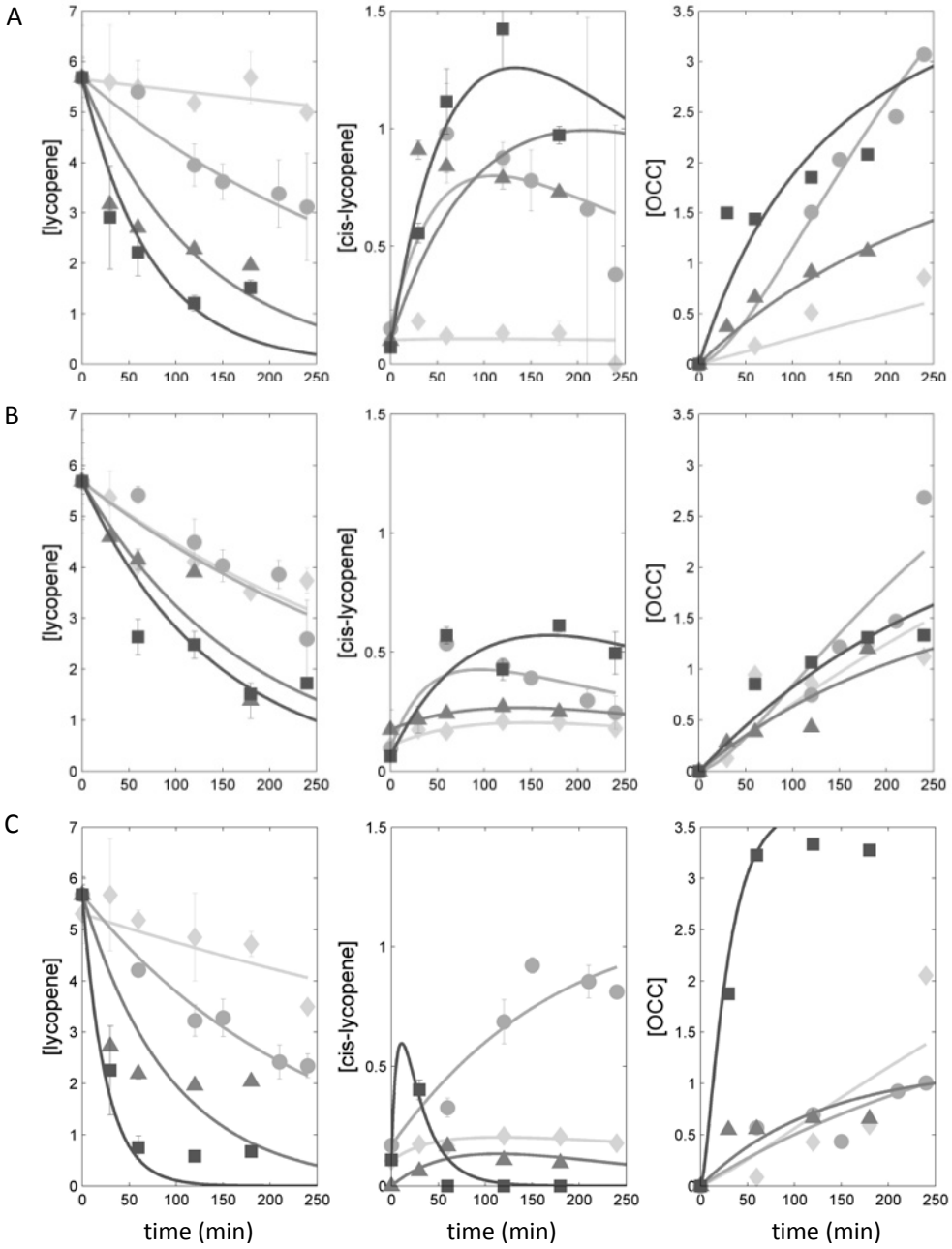

TOC GRAPHIC

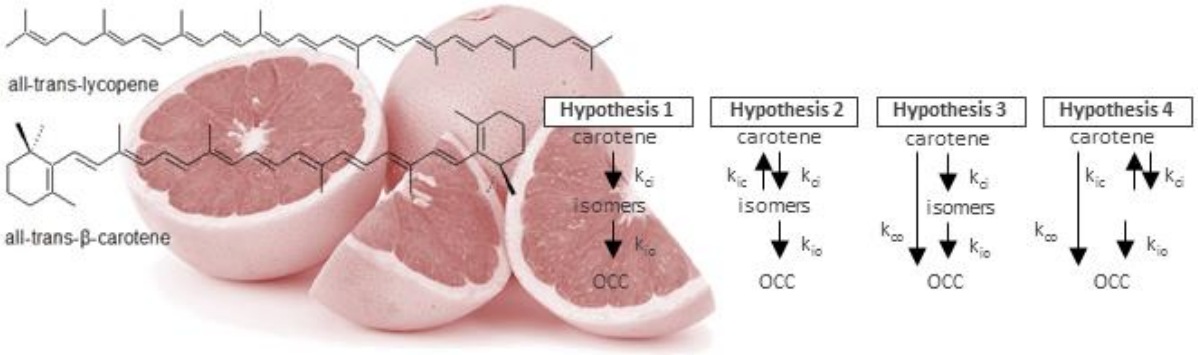
all-trans-lycopene
all-trans-β-carotene
Hypothesis 1
carotene
k_{ci}
isomers
k_{io}
OCC
Hypothesis 2
carotene
k_{ic}
k_{ci}
isomers
k_{io}
OCC
Hypothesis 3
carotene
k_{ci}
k_{∞}
isomers
k_{io}
OCC
Hypothesis 4
carotene
k_{ic}
k_{ci}
k_{∞}
k_{io}
OCC